AFRL-RZ-WP-TP-2010-2035

POLYARYLENETHIOETHERSULFONE MEMBRANES FOR FUEL CELLS (Postprint)

S.J. Rodrigues, T.L. Reitz, T.D. Dang, Z. Bai, and K. Bardua

Electrochemistry and Thermal Sciences Branch
Power Division

JANUARY 2010
Interim Report

AIR FORCE RESEARCH LABORATORY
PROPULSION DIRECTORATE
WRIGHT-PATTERSON AIR FORCE BASE, OH 45433-7251
AIR FORCE MATERIEL COMMAND
UNITED STATES AIR FORCE

REPORT DOCUMENTATION PAGE

Form Approved
OMB No. 0704-0188

1. REPORT DATE *(DD-MM-YY)*	2. REPORT TYPE	3. DATES COVERED *(From - To)*
January 2010	Journal Article Postprint	01 January 2007 – 01 May 2007

4. TITLE AND SUBTITLE
POLYARYLENETHIOETHERSULFONE MEMBRANES FOR FUEL CELLS (Postprint)

5a. CONTRACT NUMBER
IN HOUSE

5b. GRANT NUMBER

5c. PROGRAM ELEMENT NUMBER
62203F

6. AUTHOR(S)
S.J. Rodrigues and T.L. Reitz (Power Division, Electrochemistry and Thermal Sciences Branch (AFRL/RZPS))
T.D. Dang (Nonmetallic Materials Division, Polymer Branch (AFRL/RXBP))
Z. Bai (University of Dayton Research Institute)
K. Bardua (University of Dayton)

5d. PROJECT NUMBER
3145

5e. TASK NUMBER
01

5f. WORK UNIT NUMBER
314501CK

7. PERFORMING ORGANIZATION NAME(S) AND ADDRESS(ES)

Power Division, Electrochemistry and Thermal Sciences Branch (AFRL/RZPS)
Air Force Research Laboratory, Propulsion Directorate
Wright-Patterson Air Force Base, OH 45433-7251
Air Force Materiel Command
United States Air Force

Nonmetallic Materials Division, Polymer Branch (AFRL/RXBP)
Air Force Research Laboratory
Materials & Manufacturing Directorate

University of Dayton Research Institute

University of Dayton

8. PERFORMING ORGANIZATION REPORT NUMBER
AFRL-RZ-WP-TP-2010-2035

9. SPONSORING/MONITORING AGENCY NAME(S) AND ADDRESS(ES)

Air Force Research Laboratory
Propulsion Directorate
Wright-Patterson Air Force Base, OH 45433-7251
Air Force Materiel Command
United States Air Force

10. SPONSORING/MONITORING AGENCY ACRONYM(S)
AFRL/RZPS

11. SPONSORING/MONITORING AGENCY REPORT NUMBER(S)
AFRL-RZ-WP-TP-2009-2035

12. DISTRIBUTION/AVAILABILITY STATEMENT
Approved for public release; distribution unlimited.

13. SUPPLEMENTARY NOTES
PAO Case Number: 88ABW-2007-1713; Clearance Date: 24 July 2007. Published in the Journal of the Electrochemical Society, 154 (9) B960-B968 (2007).

14. ABSTRACT
High-performance sulfonated polyarylenethioethersulfone (SPTES) polymers have been developed as membranes for fuel cells. These high-molecular-weight polymers synthesized by a polycondensation process have an aromatic backbone along with high sulfonic acid content that provides for their high conductivity and robust mechanical properties. Bulky phenyl-based endcapping agents are incorporated into the system to maintain high water stability and retain high proton conductivity. Films with good mechanical properties were obtained by solvent casting. SPTES polymer systems with a 50% degree of sulfonation (SPTES-50) exhibited high proton conductivity (>100 mS/cm) at 65 °C and 85% relative humidity. Membrane electrode assemblies (MEAs) fabricated using SPTES-50 electrolytes that incorporate conventional electrode application techniques have shown high proton mobility. Electrochemical evaluation was performed using nonlinear regression analysis to obtain Tafel parameters.

15. SUBJECT TERMS
Proton exchange fuel cell, polymer

16. SECURITY CLASSIFICATION OF:			17. LIMITATION OF ABSTRACT:	18. NUMBER OF PAGES	19a. NAME OF RESPONSIBLE PERSON (Monitor)
a. REPORT	b. ABSTRACT	c. THIS PAGE			Stanley Rodrigues
Unclassified	Unclassified	Unclassified	SAR	16	19b. TELEPHONE NUMBER *(Include Area Code)* N/A

Standard Form 298 (Rev. 8-98)
Prescribed by ANSI Std. Z39-18

Journal of The Electrochemical Society, **154** (9) B960-B968 (2007)
0013-4651/2007/154(9)/B960/9/$20.00 © The Electrochemical Society

Polyarylenethioethersulfone Membranes for Fuel Cells

S. J. Rodrigues,[a,*,z] T. L. Reitz,[a,*] T. D. Dang,[b] Z. Bai,[c] and K. Bardua[d]

[a]*Air Force Research Laboratory/PRPS, Electrochemistry and Thermal Sciences Branch and* [b]*Air Force Research Laboratory/MLBP, Material and Manufacturing Directorate, Wright-Patterson Air Force Base, Ohio 45433, USA*
[c]*University of Dayton Research Institute, Dayton, Ohio 45469, USA*
[d]*University of Dayton, Dayton, Ohio 45469, USA*

High-performance sulfonated polyarylenethioethersulfone (SPTES) polymers have been developed as membranes for fuel cells. These high-molecular-weight polymers synthesized by a polycondensation process have an aromatic backbone along with high sulfonic acid content that provides for their high conductivity and robust mechanical properties. Bulky phenyl-based endcapping agents are incorporated into the system to maintain high water stability and retain high proton conductivity. Films with good mechanical properties were obtained by solvent casting. SPTES polymer systems with a 50% degree of sulfonation (SPTES-50) exhibited high proton conductivity (>100 mS/cm) at 65°C and 85% relative humidity. Membrane electrode assemblies (MEAs) fabricated using SPTES-50 electrolytes that incorporate conventional electrode application techniques have shown high proton mobility. Electrochemical evaluation was performed using nonlinear regression analysis to obtain Tafel parameters. The electrochemical performance of SPTES-50 was comparable to Nafion. Electrochemical impedance spectra were analyzed in terms of a pore-diffusion model. Catalyst utilization for SPTES MEAs using conventional electrode inks with perfluorinated binders was similar to that exhibited by Nafion. Estimates of hydrogen-fuel permeability based upon measured open-circuit voltage indicate that SPTES-50 MEAs exhibit a slightly higher rate of fuel crossover compared to Nafion. Thermogravimetric analysis shows good thermal stability. The high-temperature stability (up to 250°C) and high intrinsic proton conductivities of SPTES-50 qualify it to be a potential candidate for membranes in fuel cells.
 [DOI: 10.1149/1.2755881]

Manuscript submitted November 17, 2006; revised manuscript received May 17, 2007. Available electronically July 23, 2007.

Proton exchange membrane fuel cells (PEMFCs) are an attractive power source due to their energy efficiency and environmental compatibility.[1] Organic proton exchange membranes (PEMs) are used as electrolytes and fuel separators and are one of the most critical components[2] in these types of fuel cells.

Perfluorinated polymer membranes sold under the trademark of Nafion by DuPont have become the commercially available standard in PEMFC technology.[3,4] Nafion membranes have a polytetrafluoroethylene (PTFE) backbone, which provides thermal and chemical stability, and perfluorinated side chains with terminating sulfonic acid groups ($-SO_3H$), which aggregate and facilitate hydration, further aiding in proton conduction. On a nanometer scale the PTFE-like backbone is hydrophobic and the sulfonic acid group is hydrophilic.[5] Protons migrate through the hydrophilic phase from anode to cathode with a relatively high conductivity of 80 mS/cm.[6,7] In spite of being state-of-the-art material for PEMs, the perfluorinated ionomer membrane has some drawbacks for fuel cell applications, because the proton conductivity of the membrane strongly depends upon water and the relative humidity to hydrate ionic clusters. Thus, it has performance limitations at temperatures higher than 80°C and at low humidity levels.[8,9] An additional drawback is its high cost due to the extensive chemistry required for synthesis.

Hydrocarbon polymers are particularly attractive because they are less expensive than perfluorinated ionomers. Hydrocarbon polymers containing polar groups retain high amounts of water over a wide temperature range. Several nonfluorinated ionomer membranes have been investigated. These efforts have resulted in the development of aromatic polymers such as poly(ether ether ketone) (PEEK), poly(ethersulfone) (PES), polyphenylquinoxaline (PPQ), and polybenzimidazole (PBI).[10-14] Acid-doped PBI-based membranes have also been extensively investigated.[15,16] The hydration capabilities, high thermo-oxidative stabilities, and high strength of the benzimidazole heterocycle render them suitable as PEMs for high-temperature applications.[12]

The synthesis and characterization of high-performance polymers based on arylene ether sulfone, and thioether linkages in the backbone have been described in the literature.[17-20] These sulfonated high-performance polymers exhibit excellent thermal stability, mechanical integrity, chemical resistance, and proton conductivity and are considered good candidates for fuel cell applications. The performance limitations of Nafion can be overcome by these sulfonated polymers, especially at elevated temperatures.

The objective of this work was to develop a new class of improved and economical hydrocarbon PEMs for fuel cell applications. The approach employed was to utilize wholly aromatic polymer backbone and incorporate a pendant acid functionality directly onto the polymer backbone. A wholly aromatic backbone with high sulfonic acid content is expected to enhance water retention, which further enhances ionic conduction. The purpose of this study was to evaluate high-molecular-weight endcapped sulfonated polyarylenethioethersulfone (SPTES) polymers that form tough films, have good thermomechanical and chemical stabilities, and exhibit high conductivities for potential application in membrane electrode assemblies (MEAs) used in fuel cells.

Experimental

Materials.— The 4,4′-thiobisbenzenethiol, anhydrous potassium carbonate, and 4-fluorophenylsulfone were obtained from Aldrich and used as-received. The 3,3′-disulfonate-4,4′-difluorodiphenylsulfone monomer,[20,21] was prepared by the sulfonation reaction of 4-fluorophenylsulfone with sulfuric acid.

Monomer synthesis.— The 4-fluorophenylsulfone (25.4 g, 0.1 mol) was mixed with 50 mL of 30% fuming sulfuric acid in a 100 mL, single-necked flask equipped with a magnetic stirrer and a drying tube. The mixture was heated to 160°C for 12 h to produce a homogeneous solution and then poured into 300 mL of ice water under stirring. Next, a 4 M aqueous solution of sodium hydroxide was added, which changed the pH to 7. Sodium chloride (120 g) was added to obtain a sodium-form of the disulfonated monomer. The crude product was filtered and recrystallized from a heated mixture of isopropanol and deionized water (80:20 v/v) to produce fine, white crystals after drying overnight in a vacuum oven. The yield after crystallization was 91%.

Polymer synthesis.— Synthesis of endcapped SPTES-50 copolymer was performed via step-growth copolymerization. The reaction was carried out in a 250 mL three-neck round-bottom flask equipped with a mechanical stirrer and a nitrogen inlet-outlet. The 3,3′-disulfonate-4,4′-difluorodiphenylsulfone (4.5833 g, 0.01 mol),

* Electrochemical Society Active Member.
z E-mail: stanley.rodrigues@wpafb.af.mil

4-fluorophenylsulfone (2.54 g, 0.01 mol), 4,4′-thiobisbenzenethiol (5.0082 g, 0.02 mol), and anhydrous potassium carbonate (5.8048 g, 0.042 mol) were charged into the flask under nitrogen pressure. Following this, 120 mL of sulfolane was added into the flask, stirred for 30 min at room temperature, and then heated to 100°C for 1 h using an oil bath on a hot plate. The 4-fluorobenzophenone (0.0001 mol) was added to the solution and the reaction mixture was heated to 160–180°C for 4–5 h. The viscous reaction solution was cooled down to room temperature, quenched with acetic acid in methanol, and the sulfonated copolymer was isolated in stirred methanol. The precipitated copolymer was washed several times with deionized water in an attempt to completely remove the salts and then soxhlet-extracted in methanol for 72 h. Finally, it was vacuum dried at 100°C for 24 h with a yield of 92%. Copolymer compositions with high sulfonic acid content (50–100% sulfonated repeat unit) and bulky endgroups were readily synthesized using this methodology.

Membrane fabrication.— Membranes were prepared by dissolving the sodium-form SPTES-50 copolymer in dimethylacetamide (DMAc) (10% w/v) to obtain 5–10% transparent solution. The solution was then filtered using a 0.45 μm Teflon syringe filter to remove contaminants and cast directly onto clean glass substrates. The sodium-form membranes were carefully vacuum-dried by gradually increasing temperatures to 100°C over 24 h and further to 120°C over an additional 2 h. The drying procedure was optimized to produce flat, transparent membranes, gradually eliminating the casting solvent. Drying at a rapid rate produced membranes that were rough, brittle, and with voids. The SPTES-50 copolymer sodium-form membranes were converted into acid-form by the acidification procedure. This involved immersion of membranes for 24 h in 4 M sulfuric acid at room temperature, followed by soaking for 2–4 h in deionized water, washing with deionized water for 2 h, and vacuum drying at 80°C for 24 h. The dry membrane thickness was measured using a micrometer.

Mechanical properties.— Mechanical properties that include tensile strength, tensile modulus, and elongation were evaluated using methods based on ASTM-D882 and ASTM-1004. SPTES-50 and Nafion samples (both dry and wet) were characterized. Samples of the membranes were dried at 80°C in vacuum for 10 h prior to testing. Wet samples were immersed in deionized water at room temperature for 10 h prior to testing.

Water uptake.— Polymer membranes were dried (80°C) in a vacuum oven and weighed (W_2). The membranes were weighed (W_1) after immersion in deionized water for 2 h at various controlled temperatures. The water uptake was calculated with reference to the weight of the dry polymer membrane, i.e., $(W_1/W_2 - 1) \times 100$. For comparison, both SPTES-50 and Nafion membranes were used.

Proton conductivity.— The proton conductivity was measured by means of ac impedance spectroscopy over a frequency range of 0.1 Hz–10 MHz with a voltage of 10 mV, using a EG&G potentiostat and a frequency response analyzer. In order to eliminate electrode and interfacial effect, a standard four-probe setup was used (Fig. 1).

Current was applied to the outer two electrodes made up of platinum foil. Two inner platinum wire electrodes measured the voltage drop across a known distance. The setup was placed in a controlled temperature and humidity oven. The impedance of the samples was obtained as a function of frequency at a given temperature and humidity level. The conductivity was obtained using the magnitude of the impedance in a region where the phase angle is essentially zero.

MEA fabrication.— A painting technique was used to form the catalyst layer on both sides of the membranes using a catalyst ink slurry. This slurry consisted of platinum black (Aldrich), water, and 5% Nafion solution (1100 equivalent weight, Fluka Chemicals) as binder. The ink slurry was sonicated to break up the catalyst powder in order to obtain a homogenous distribution. Several layers of the ink were painted on both sides of the membranes. Samples were dried at 80°C under vacuum for 10 h to eliminate all solvents. The anode and cathode composition were 90 wt % platinum black and 10 wt % Nafion. The catalyst loading was approximately 5 mg/cm^2 and the geometric active area was 5 cm^2. Hydrophobic carbon cloths (E-TEK, Inc.) were used as anode and cathode gas diffusion layers to fabricate MEAs.

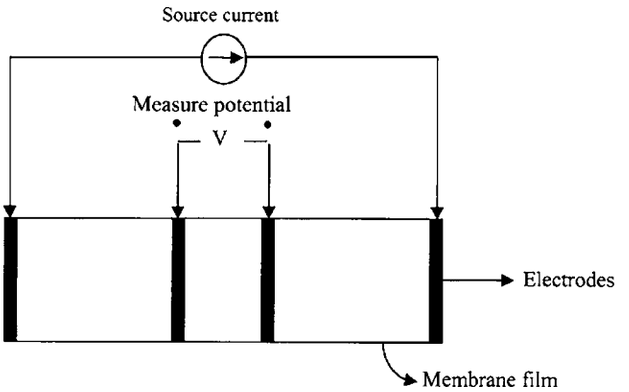

Figure 1. A four-electrode setup to measure proton conductivity.

Single-cell test (H-PEMFC).— MEAs were positioned in a single-cell fixture with graphite blocks as current collectors, having a serpentine flow pattern using a Fuel Cell Technologies, Inc. test station. The gases used (H_2, air, and O_2) were humidified, with the gas humidity bottles set at 80°C. The stoichiometric ratio for the fuel gas and oxidant was 2.5 based on the consumption rate at 1 A/cm^2. Humidity was verified with an in-line high-temperature humidity probe. Cell performance was obtained at 1 atmosphere with cell temperatures at 80 and 100°C. The load (Amrel Systems, Inc.) used for a single-cell test is based on a field-effect transistor (FET) programmable electronic load (10 V, 50 A–max 60 W) set at constant-current mode. Polarization plots of Nafion and SPTES-50-based MEAs were obtained and compared. Life test was performed at 80°C using H_2 and air with flow rates of 200 and 500 sccm, respectively, and with 20 psig back pressure on each side.

Electrochemical impedance spectroscopy.— Electrical impedance spectroscopy (EIS) was utilized to deconvolute electrochemical losses in the fuel cell. A Solartron SI 1280 impedance/gain-phase analyzer in conjunction with SI 1287 electrochemical interface was used to determine relative impedances and interpret the physical nature of the cell structure. MEAs were examined over a frequency range of 1 MHz–0.1 Hz in a conventional two-probe mode. Information such as membrane resistance, charge-transfer resistance, and pore resistance was extracted from impedance plots using Nafion- and SPTES-50-based MEAs with H_2 as fuel and air and pure O_2 as oxidants.

Microscopy.— The morphology of a single MEA was investigated using a scanning electrode microscope (SEM).

Results and Discussion

The polymer compositions described here involve the incorporation of bulky endcaps. Using endcaps profoundly modifies polymer properties such as solubility and swelling, provides viable copolymer compositions with high sulfonic acid content (50–100% sulfonated repeat unit), and helps narrow molecular weight distribution. This methodology provides a departure from the copolymer compositions described by Wang et al.[20]

SPTES-50 copolymers synthesized with endcapping groups (Fig. 2) were fabricated into transparent films with an average thickness

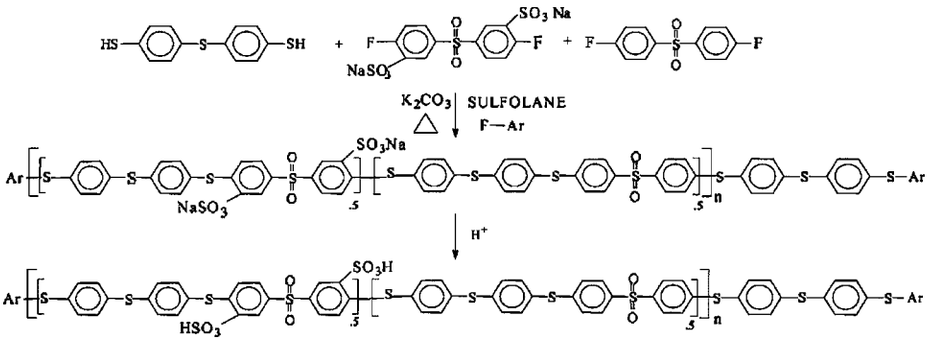

Figure 2. Synthesis of acid-form SPTES-50.

of 5 mils. One of the merits of direct copolymerization of sulfonated monomers is enhanced stability due to the deactivated position of the -SO_3H group. Conversion of the sodium-form membranes to acid-form membranes was confirmed through thermogravimetric analysis (TGA), as shown in Fig. 3. There is no residue for the acid-form sample at temperatures above 600°C, whereas the char yield is greater than 30% for the salt-form sample. As expected, the sodium-form materials have enhanced thermal stability relative to the acid form. The degradation of sulfonic acid pendants on the salt-form SPTES-50 backbone was in the temperature range of 400–500°C, whereas the degradation of the corresponding free acid-form was in the range of 200–300°C. The ion-exchange capacity (IEC) of SPTES-50 membranes was found to be 1.64 meq/g using a reverse-titration technique, compared to 0.91 meq/g for commercial Nafion using the same technique.

Mechanical strength of membrane affects manufacturing conditions of MEAs and durability of PEMFCs. Table I shows tensile strength at yield and at break for dry and wet samples. In all conditions, SPTES-50 membranes exhibited greater strength than Nafion. Upon hydration Nafion lost a large part of its strength, whereas the loss for SPTES-50 was modest. SPTES-50 membranes are also stiffer than Nafion as reflected by the larger tensile modulus values. Thus, SPTES-50 is mechanically superior to Nafion. Additional characterizations of SPTES-50 that include TGA, intrinsic viscosity, and molecular weight have been discussed elsewhere.[22,23]

The purpose of sulfonation is to increase the acidity and hydrophilicity. The proton transfer and hence conductivity of solid electrolytes is enhanced in the presence of water. The water uptake for SPTES increases with the degree of sulfonation due to its increased polarity and temperature, as shown in Fig. 4. SPTES-50 shows higher water uptake compared to Nafion. SPTES membranes, sulfonated beyond 50%, exhibit accelerated water uptake and significant swelling, which may be detrimental to its performance as electrolytes for fuel cells. Additionally, it is suspected that thermal cycling could weaken its structural integrity by making it prone to developing microcracks or pores.

Sulfonation enhances the conductivity because of the hydrophilic sulfonic groups (-SO_3H) which form water-mediated pathways for protons. The proton conductivity of endcapped SPTES-50 is shown in Fig. 5 as a function of temperature and relative humidity (RH). The four-point-probe method provides membrane resistance without the effect of charge-transfer resistance and other nonohmic resistances. Proton conductivities greater than 100 mS/cm at temperatures greater than 60°C and 85% RH are exhibited by these membranes. The endcapping group incorporated onto the polymer backbone does not significantly affect its conductivity. The function of these groups is to render the polymer insoluble in water without adversely affecting the proton conductivity. The enhancement of

Table I. Mechanical properties of dry and wet samples of Nafion and SPTES-50.

	SPTES-50		Nafion	
	Dry	Wet	Dry	Wet
Tensile strength at yield (MPa)	38	32	14.2	8.0
Tensile strength at break (MPa)	35	33	31.4	19.8
Elongation at break (%)	31.6	86.6	270	201
Tensile modulus (GPa)	1.23	0.981	0.357	0.152

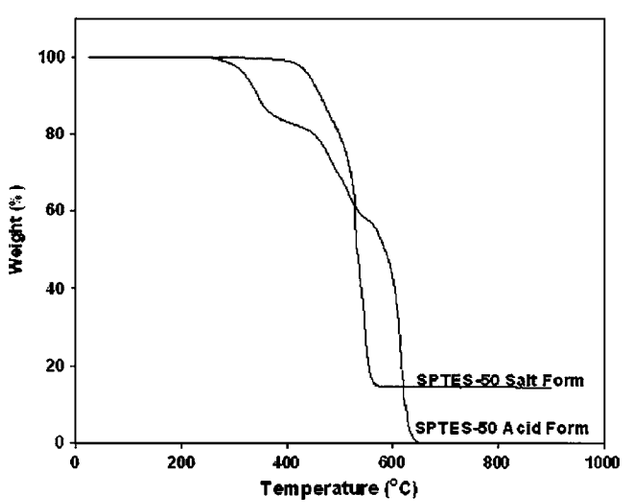

Figure 3. TGA plots of Na-form and acid-form SPTES-50 membranes in air.

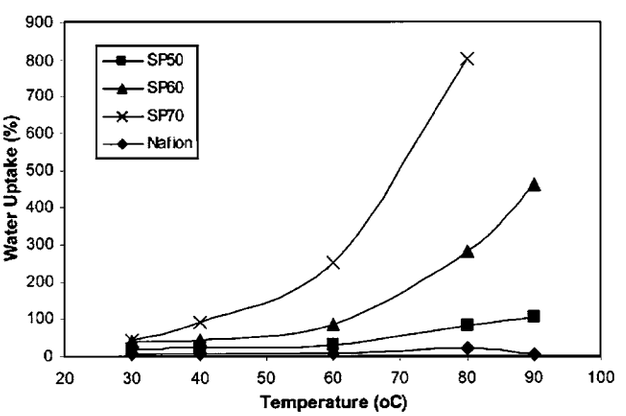

Figure 4. SPTES and Nafion water uptake as a function of temperature.

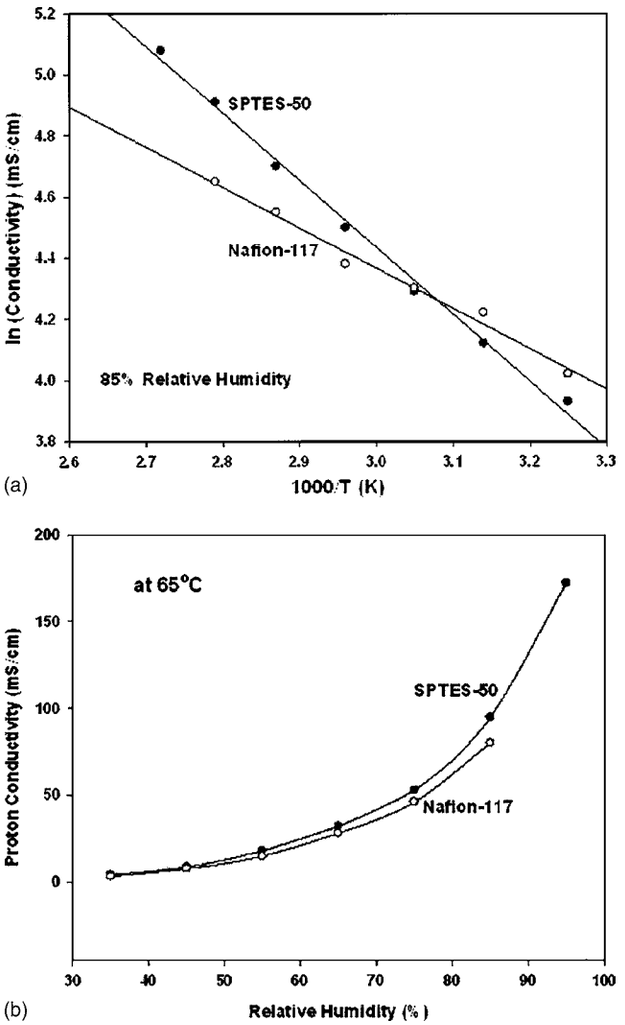

Figure 5. Proton conductivity as a function of (a) temperature (85% RH) and (b) RH (65°C).

proton conductivity is due to high proton mobility resulting from increased water uptake. The high water uptake results from increased protonated sites. The sulfonic acid per repeating unit for SPTES-50 is greater than that of Nafion. This is reflected in the IEC of SPTES-50. The calculated and measured IEC for SPTES-50 are 1.83 and 1.64 meq/g, respectively. The calculated IEC for Nafion is 0.91 meq/g. It is speculated that the proton-transport mechanism in SPTES-50 is similar to the transport mechanism of Nafion, which involves direct migration of hydronium ions (vehicle mechanism) and orientational mode assisted proton hopping (Grotthus mechanism).

The key performance measure of a fuel cell is the polarization data that relates the voltage output as a function of electrical current density drawn. The open-circuit voltage (OCV) is a mixed potential and its value is a good measure for fuel crossover (in this case, H_2 migrating through the membrane to the cathode). The OCV is determined by considering the crossover H_2 oxidation and the current density for O_2 reduction at the cathode. The average OCV for Nafion was greater compared to the OCV for SPTES-50, indicating some fuel crossover through the SPTES-50 membrane. This could be attributed to flaws/defects in the membrane structure, such as pinholes.

Electrochemical evaluation of the performance of the SPTES-50 system relative to Nafion was performed by a nonlinear regression analysis of the polarization data using Eq. 1 and 2

$$E = E_o - b \log i - iR \quad [1]$$

$$E_o = E_r + b \log i_o \quad [2]$$

The parameters b and i_o are the Tafel slope and exchange current density, respectively, and are primarily associated with the kinetics of the oxygen reduction reaction. E_r is the thermodynamic reversible potential. The combined resistance, R, is related to the linear decrease in potential as a function of current density and is primarily associated with MEA resistance, but it is also affected by the resistance of the testing apparatus. This approach has been presented in the literature and provides a good match to experimental polarization data for current densities sufficiently far from the limiting current density.[24-26] Data obtained using regression analysis for the SPTES-50 and Nafion specimens at cell temperatures of 80 and 100°C are presented in Table II.

As shown in Fig. 6, using H_2 and air at 80 and 100°C the model curve appears to fit the experimental points rather well. Overall, electrochemical performance of the STPES-50 sample is comparable to that of the Nafion. At lower temperatures (80°C), the Nafion specimen appears to exhibit better oxygen-reduction kinetics relative to the SPTES-50 specimen, with the most pronounced difference between the Tafel slopes and exchange current densities (Table II) observed when pure oxygen was used in the cathode. As discussed previously, SPTES-50 exhibited a lower OCV and E_o, which presumably is related to microporous defects in the SPTES-50 specimens that often occur during the solvent-casting process. Con-

Table II. Comparative Tafel parameters of Nafion and SPTES-50.

Specimen (anode/cathode)	Cell temp (°C)	OCV (mV)	E_o (mV)	b (mV/dec)	i_o (mA/cm^2)	R (Ω cm^2)	ASR (Ω cm^2)
Nafion 115 (H_2/air)	80	1007	998.1	60	2.3×10^{-4}	0.43	0.16
SPTES-50 (H_2/air)	80	950	949	41	4.0×10^{-7}	0.40	0.15
Nafion 115 (H_2/air)	100	973	930	49	1.9×10^{-6}	1.16	0.73
SPTES-50 (H_2/air)	100	950	945	69	1.4×10^{-4}	1.28	0.80
Nafion 115 (H_2/O_2)	80	1006	1002	58	2.6×10^{-4}	0.29	0.18
SPTES-50 (H_2/O_2)	80	940	948	28	4.4×10^{-10}	0.33	0.16
Nafion 115 (H_2/O_2)	100	1000	1002	72	1.3×10^{-3}	0.83	0.65
SPTES-50 (H_2/O_2)	100	900	907	44	1.0×10^{-7}	0.77	0.80

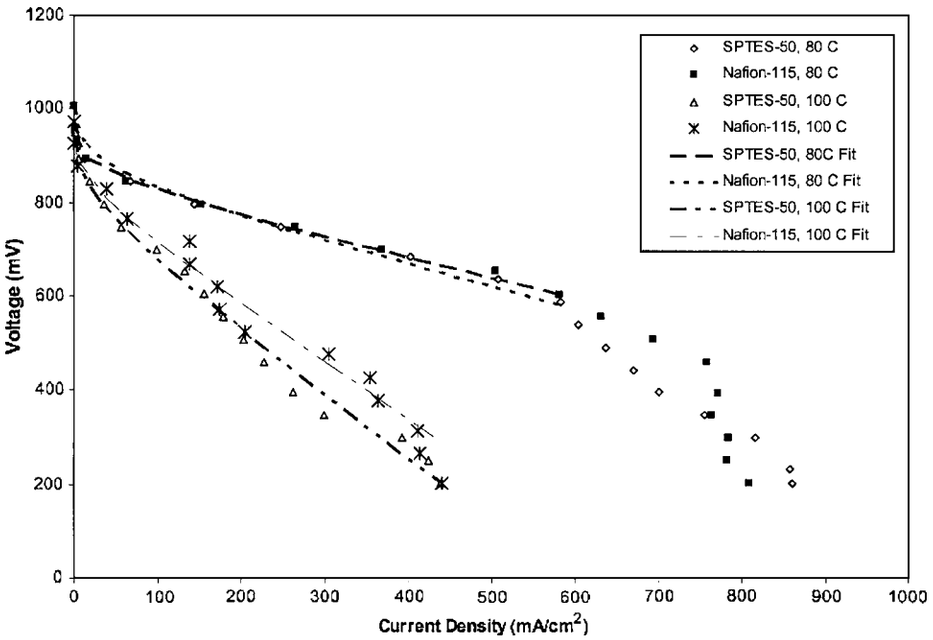

Figure 6. Polarization plots (data and fit) of Nafion and SPTES-50 using H_2 and air at different temperatures.

ductivity, as measured by the high-frequency resistance using area specific resistance (ASR) and as determined via simulation (R), appears to be better in the SPTES-50 specimen, but uncertainties in the data make absolute determination difficult. Absolute conductivity of the SPTES-50 polymer electrolyte specimen has been observed to be significantly better than Nafion (Fig. 5).

Polarization curves alone do not allow for a complete understanding of the relative differences between PEM systems. Competing processes which include catalyst activity, interfacial resistance, and diffusion processes all occur to different extents and contribute to losses observed in a polarization curve. In order to assess the relative contribution of these losses over a range of current densities, EIS can be employed, which allows for the exploitation of the various processes. Table III displays some of these processes and their respective time scales. For example, if a proper experiment can be performed, it is possible to deconvolute the relative extent of electrode catalyst inefficiencies from reactant diffusion resistance by probing their relative impedances at different frequencies. These impedance spectra can be mathematically modeled through the use of standard resistance-capacitance (RC) circuit elements wherein resistors can be used in conjunction with capacitive elements to approximate both real and imaginary impedances. Additional factors can adversely affect performance efficiencies, resulting in deviations from ideality which includes fuel crossover losses and irregularities due to anisotropic membranes. These inefficiencies are not readily obvious by examination of either the polarization curve or an impedance spectrum and must be evaluated by other characterization means.

Table III. Various impedances and their time scales.

Processes	Description	Time (s)
Electron mobility	Electrons motion in electrodes and through interfaces	$<10^{-6}$
Ionic conductivity	Movement of ions through electrolyte	$\sim 10^{-5}$–10^{-3}
Activation	Reaction rate effect	$\sim 10^{-3}$–10^{-1}
Concentration	Reactants diffusion through electrodes and flow fields	$>10^{-1}$

Impedance spectra of both SPTES-50 and Nafion MEAs were obtained at three polarizations, OCV, 0.9, and 0.8 V, in order to elucidate performance parameter differences between the PEM systems. The current densities at 0.9 and 0.8 V were 14 and 146 mA/cm^2, respectively, for SPTES-50 and 14 and 148 mA/cm^2, respectively, for Nafion using H_2 and air. The current densities at 0.9 and 0.8 V were 26 and 230 mA/cm^2, respectively, for SPTES-50 and 24 and 220 mA/cm^2, respectively, for Nafion using H_2 and O_2. These polarizations were selected to allow elucidation primarily of the activation polarization and kinetic parameters relating to the differences between the electrolytes. Higher polarizations from OCV were not studied because diffusion limitations were assumed to be constant for both systems because the application and electrode materials were identical in both systems. In order to better understand the extent to which the cathode impedances impact the different electrolyte systems, gas composition was also varied to include humidified air and oxygen.

Figures 7 and 8 are typical Nyquist plots for various polarizations of Nafion and SPTES-50 PEMs obtained under H_2/air and H_2/O_2 environments, respectively. These Nyquist plots seem to indicate that the electrochemical performances of the two electrolytes are similar with primary (high-frequency) intercepts occurring at approximately the same location on the real impedance axis (Z'). The most obvious feature in the Nafion and SPTES-50 H_2/air spectra at bias potentials is a single, distorted semicircle, the center of which lies below the real axis into the positive Z'' region. Closer inspection, however, seems to show evidence of two overlapping semicircles, the high-frequency component of which is presumably related to effective pore-diffusion resistance and double-layer capacitance in the catalyst/electrolyte interface. The low-frequency feature has historically been attributed primarily to mass transport of oxygen in the cathode gas diffusion layer but can also be attributed to charge-transfer resistance in porous electrodes.[27] No Warburg impedances were observed in either system, suggesting that no obvious diffusion limitations occurred. This is not surprising, however, given that the impedance spectra were not taken at extremely high polarizations where one might expect to see these features. The differences in the spectra for the samples are more pronounced at the lower frequency range, with impedance curves measured at no polarization (open circuit) exhibiting the most significant difference. As would be anticipated, lower frequency intercepts are obvious

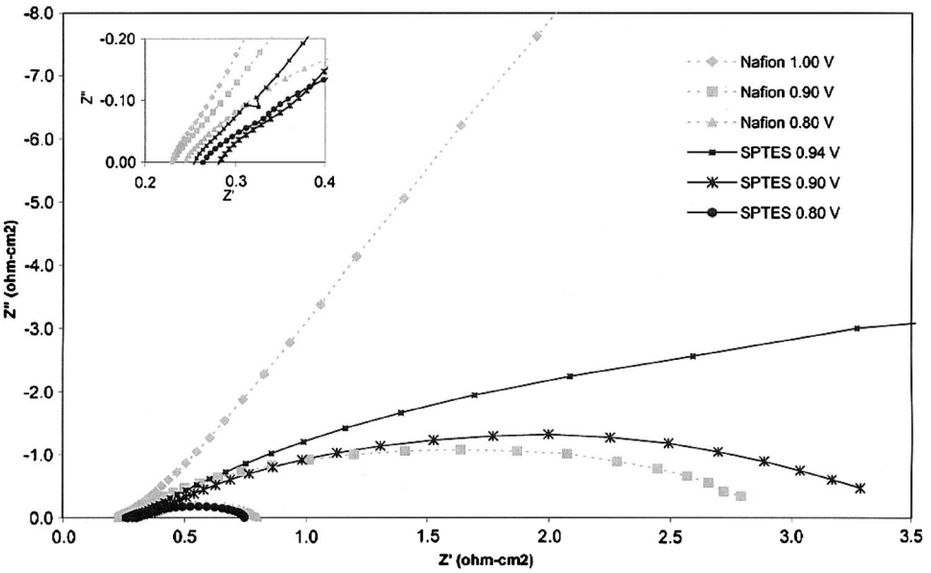

Figure 7. Impedance plots at various polarization potentials of Nafion and SPTES-50 MEAs using H_2/air at 80°C.

functions of both reactant gas-phase composition and polarization. This can be attributed to the likelihood that the low-frequency features are due to differences in activation polarization, primarily located at the cathode. This is particularly obvious when pure oxygen is fed into the cathode. A comparison of Fig. 7 and 8 shows that significant reductions in both real and imaginary impedances occur when oxygen is used instead of air, especially for the lower frequency features. When pure oxygen is used in the cathode for the Nafion when oxygen is used instead of air specimen, a noticeable second semicircle begins to appear at the lower frequency, which suggests that these lower frequency features are related to enhanced oxygen diffusion in the gas diffusion layers. As such, small differences in the manner in which the particular electrolyte interacts with the gas diffusion electrode can result in pronounced differences in the interfacial impedances.

In order to better understand the nature and extent of the different electrochemical impedances of the competing systems, the various spectra were fit to different RC circuit models. Best attempts were made to select electrochemical elements and RC circuits which had been shown in literature to have a reasonable physical interpretation.[28-30] Ultimately, it was observed that a modified pore diffusion model, which incorporates constant phase elements (CPEs) in lieu of standard capacitive elements, most accurately represented the entire data set (Fig. 9). This model seeks to approximate impedance spectra by fitting the data to three discrete elements with differing time constants. These elements have been shown to appropriately model electrochemical behavior in porous electrodes, including intraparticle diffusion resistance, sorption/reaction phenomenon on the catalyst site, and electrical resistance in the electrode assembly. CPEs are mathematically similar to a standard capacitor except that an additional parameter (α) is added which allows for these deviations from ideality (Eq. 3 and 4)

$$Z_c = 1/C\varpi j \quad [3]$$

$$Z_{CPE} = 1/C(\varpi j)^{\alpha} \quad [4]$$

In this effort, α primarily ranged from 0.85 to 1, which is typical for the distributed element behavior observed in porous electrodes.

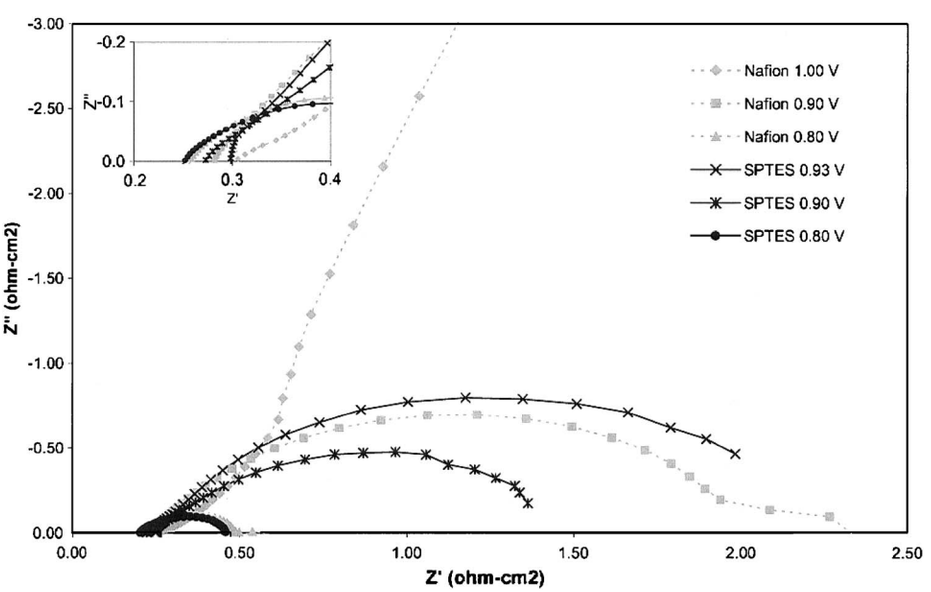

Figure 8. Impedance plots at various polarization potentials of Nafion and SPTES-50 MEAs using H_2/O_2 at 80°C.

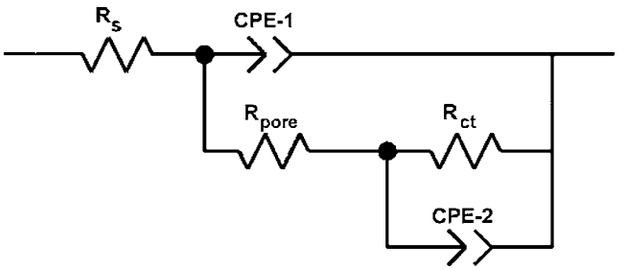

Figure 9. Pore-diffusion model used in the electrochemical impedance analysis.

The EIS data regressed using the porous-electrode-circuit model and is presented in Tables IV and V for both Nafion and SPTES-50 electrolyte MEAs under air and O_2 atmospheres. Additionally, ASRs are also presented for both systems. Resistance R_s is directly related to the MEA resistance and was observed to agree with the ASR. Despite the low ASR of the SPTES-50 electrolyte relative to Nafion, the observed MEA resistance R_s appeared to be similar in both specimens. This is because the resistance of the electrolyte is not significant relative to the impedance associated with the gas diffusion electrodes (GDEs), catalyst layers, and the interfacial. The parameter Z_{cl}, generally referred to as the geometric capacitance, did not appear to be a function of gas-phase concentration or cell potential and is assumed to be primarily related to the combined capacitive contribution of the cell. The impedance for the second time constant has historically been associated with resistance in the porous electrode which, while it should be influenced by cathode oxygen partial pressure, was observed not to be significantly related within error.[30] This inconsistency is likely explained by the significant difficulty in determining the second real intercept primarily due to the distributed elements. The last two circuit elements Z_{cGC} and R_{ct} were assumed to be related to the Gouy–Chapman diffuse double-layer capacitance and charge-transfer resistance in the catalyst layer, respectively. Both R_{ct} and Z_{cGC} were determined to be significant functions of polarization and cathode oxygen concentration, which is consistent with their relationship to the kinetic parameters primarily associated with the oxygen reduction reaction. It was initially speculated that because a Nafion ink was used as the binder material in the catalyst layers of both SPTES-50 and Nafion MEAs, a preferential interface would be promoted on the Nafion electrolyte because of the similar perfluorinated chemistries. However, there does not appear to be a significant difference between the SPTES-50 and Nafion as measured by the R_{ct} or Guoy–Chapman capacitance to substantiate this hypothesis.

When the polarization data are considered universally it becomes obvious that the SPTES-50 specimen, while being intrinsically more conductive than the Nafion, does not exhibit significantly better low-temperature performance. This is likely because conventional electrode application techniques were used to prepare both SPTES-50 and Nafion MEAs. In this process, Nafion binder was used in the catalyst ink and the interfacial resistance for Nafion MEAs was expected to decrease. However, it appears that the disparate chemistries between the Nafion perfluorinated ink and the hydrocarbon-based SPTES-50 do not provide an efficient electrode/electrolyte interface. This hypothesis is substantiated upon careful inspection of an SEM microscopy image (Fig. 10) of the SPTES-50, wherein obvious cracks appear at the interface between the catalyst layer and the SPTES electrolyte. These features indicate a less-efficient electrode-electrolyte interface. Regardless, it is apparent that alternative ink formulations must be explored to improve the bonding of the electrodes onto the hydrocarbon-based polymer electrolyte.

The morphology of an SPTES-50 MEA along with elemental mapping is shown in Fig. 11. The presence of fluorine is due to the Nafion binder used in the preparation of the ink slurry to fabricate electrodes on the SPTES-50 membranes. The uniform distribution of sulfur indicates homogeneous distribution of the sulfonated system. The platinum catalyst appears to be unevenly distributed on both sides of the membrane. This is attributed to the manual application of the electrode ink slurry. The interface between the membrane and catalyst layer reveals significant defects that most likely occurred either during MEA preparation or during the operation of the single cell, indicating that the fabrication process needs to be optimized.

Life test (Fig. 12) was performed by operating at a constant cell voltage of 0.5 V and monitoring the current density as a function of time. The cell temperature was held at 80°C and the anode and cathode humidification temperatures were 105 and 90°C, respectively. The cell operation was periodically stopped every 24 h and restarted. The OCV was recorded at the start of every cycle. A total of 16 start-stop cycles were applied, with a total testing time of 400 h. The cell resistance remained unchanged ($0.127\ \Omega\ cm^2$) and the performance was sustainable for 400 h without catastrophic failure. However, the cell performance was significantly reduced (Fig.

Table IV. Impedance parameters for Nafion and SPTES-50 MEAs using H_2/air at 80°C.

Specimen	Polarization potential (V)	ASR ($\Omega\ cm^2$)	R_s ($\Omega\ cm^2$)	Z_{c1} (F/cm^2)	α_1	R_{pore} ($\Omega\ cm^2$)	R_{ct} ($\Omega\ cm^2$)	Z_{cGC} (F/cm^2)	α_2
Nafion	OCV	0.16	0.14	0.06	0.89	0.48	-	0.05	0.84
	0.9		0.14	0.05	0.88	0.21	2.43	0.07	0.87
	0.8		0.15	0.08	0.82	0.20	0.36	0.07	0.90
SPTES-50	OCV	0.15	0.16	0.07	0.79	0.23	6.61	0.08	0.83
	0.9		0.19	0.03	0.83	0.22	3.73	0.10	0.78
	0.8		0.17	0.07	0.78	0.21	0.29	0.10	0.95

Table V. Impedance parameters for Nafion and SPTES-50 MEAs using H_2/O_2 at 80°C.

Specimen	Polarization potential (V)	ASR ($\Omega\ cm^2$)	R_s ($\Omega\ cm^2$)	Z_{c1} (F/cm^2)	α_1	R_{pore} ($\Omega\ cm^2$)	R_{ct} ($\Omega\ cm^2$)	Z_{cGC} (F/cm^2)	α_2
Nafion	0	0.18	0.14	0.03	0.87	0.94	-	0.01	0.84
	0.9		0.14	0.04	0.89	0.19	1.59	0.06	0.83
	0.8		0.12	0.12	0.79	0.19	0.10	0.01	0.94
SPTES-50	0	0.16	0.16	0.02	0.98	0.16	1.88	0.08	0.83
	0.9		0.13	0.05	0.8	0.22	1.06	0.05	0.84
	0.8		0.11	0.07	0.83	0.15	0.11	0.09	0.99

Figure 10. SEM micrograph of (a) SPTES-50 and (b) Nafion MEAs.

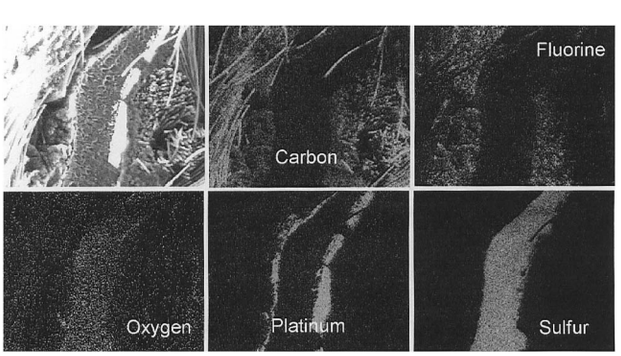

Figure 11. SPTES-50 MEA morphology and elemental analysis.

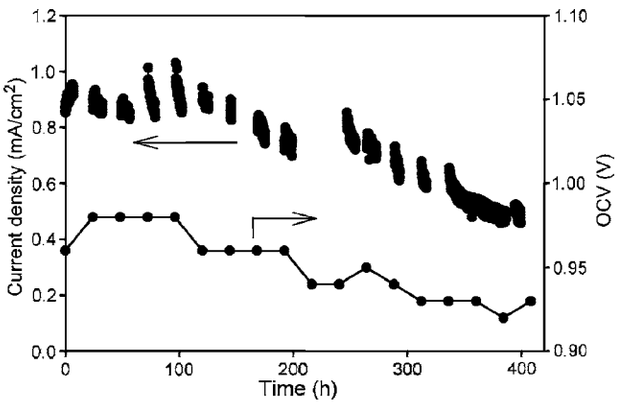

Figure 12. Current density and OCV during start-stop life test.

13). The performance loss is most likely attributed to the loss of active catalyst surface area caused by both agglomeration of catalysts and detachment of clusters from the catalyst-layer surface, possibly by ionomer dissolution. Also, a change of porosity and tortuosity of the catalyst layer reduces catalyst utilization, thereby decreasing performance. Another possibility for the loss of performance is the decrease in the gas diffusion layer hydrophobicity.

As the OCV is a mixed potential, determined by the current density for O_2 reduction and the crossover-fuel oxidation, the value of the OCV is a good indicator of fuel crossover. The OCV decreased from 0.96 V at the beginning of the test to 0.93 V at the end of the test, indicating membrane thinning and/or generation of pinholes, enhancing hydrogen crossover. The rate of voltage loss is approximately 75 μV/h. A loss rate of <1 μV/h is desirable for potential application of this membrane system.

A postmortem inspection after the life test revealed increased brittleness of the membrane caused by nonuniform physical degradation. Further investigation is necessary for any decisive conclusions about membrane degradation.

Conclusion

Low-cost, hydrocarbon-based SPTES-50 polymer membranes with endcapping groups were synthesized and characterized. These

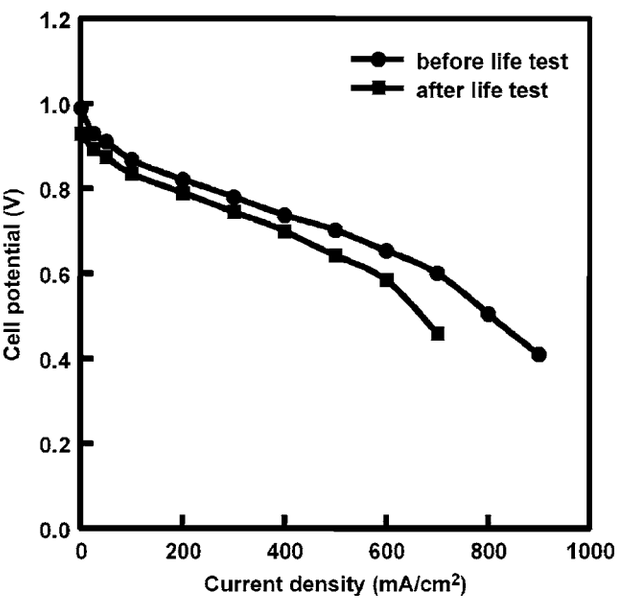

Figure 13. Polarization curves before and after start-stop life test.

high-molecular-weight polymers were readily fabricated into tough films in their acid form. SPTES-50 exhibited high proton conductivity (>100 mS/cm) at 65°C and 85% RH. The bulky aromatic endcapping groups rendered the polymers stable in water while still maintaining their proton conductivity. Operational MEAs were successfully fabricated based on these PEMs. Overall fuel cell performance, based on current material processing, was on par with Nafion at both low and high temperatures and the potential exists for enhancing the performance. The number of reaction sites on the SPTES-50 electrolyte and electrode interface appears to be more active. The higher intrinsic conductivity also accounts for the high performance of the membrane in a fuel cell. However, life test shows performance loss. Further research is needed to elucidate membrane degradation and failure mechanisms to improve lifetime performance.

Acknowledgments

The authors express appreciation to Dr. Y. S. Kim (Los Alamos National Laboratory) for the life test.

The Air Force Research Laboratory assisted in meeting the publication costs of this article.

References

1. K. Kordesch and G. Simader, *Fuel Cells and Their Applications*, VCH, Weinheim (1996).
2. J. A. Kerres, *J. Membr. Sci.*, **185**, 3 (2001).
3. C. Gavach and G. Pourcelly, *Proton Conductors: Solids, Membranes and Gels-Material and Devices*, Cambridge University Press, Cambridge, MA (1992).
4. T. A. Zawodzinski, V. T. Smith, and S. Gottesfeld, *J. Electrochem. Soc.*, **140**, 1041 (1993).
5. T. D. Gierke, G. E. Munn, and F. C. Wilson, *J. Polym. Sci., Polym. Lett. Ed.*, **19**, 1687 (1981).
6. M. Peneri and A. Eisenburg, *Structure and Properties of Ionomers*, NATO ASI Series 198, Reidel Publishing Company, Dordrecht, The Netherlands (1987).
7. S. R. Samms, S. Wasmus, and R. F. Savinell, *J. Electrochem. Soc.*, **143**, 1498 (1996).
8. Y. Sone, P. Ekdunge, and D. Simonsson, *J. Electrochem. Soc.*, **143**, 1254 (1996).
9. P. Dimitrova, K. A. Friedrich, U. Stimming, and B. Vogt, *Solid State Ionics*, **150**, 115 (2002).
10. R. W. Kopitzke and C. A. Linkous, *J. Electrochem. Soc.*, **147**, 1677 (2000).
11. S. M. J. Zaidi, S. D. Mikhailenko, G. P. Robertson, M. D. Guiver, and S. Kaliaguine, *J. Membr. Sci.*, **173**, 17 (2000).
12. J. S. Wainright, J. T. Wang, and D. Weng, *J. Electrochem. Soc.*, **142**, L121 (1995).
13. M. Kawahara, M. Rikekawa, and K. Sanui, *Solid State Ionics*, **136**, 1193 (2000).
14. A. Schechter and R. F. Savinell, *Solid State Ionics*, **147**, 1815 (2002).
15. B. Xing and O. Savadogo, *J. New Mater. Electrochem. Syst.*, **2**, 95 (1999).
16. O. Savadogo and B. Xing, *J. New Mater. Electrochem. Syst.*, **3**, 345 (2000).
17. M. Ueda, H. Toyota, and T. Teramoto, *J. Polym. Sci., Part A: Polym. Chem.*, **31**, 853 (1993).
18. C. Allam, K. J. Liu, and D. K. Mohanty, *Macromol. Chem. Phys.*, **200**, 1854 (1999).
19. F. Wang, M. Hickner, Q. Ji, W. Harrison, J. Mecham, and J. E. McGrath, *Polym. Prepr. (Am. Chem. Soc. Div. Polym. Chem.)*, **41**, 237 (2000).
20. F. Wang, M. Hickner, Y. S. Kim, T. A. Zawodzinski, and J. E. McGrath, *J. Membr. Sci.*, **197**, 231 (2002).
21. F. Wang, M. Hickner, Q. Ji, W. Harrison, J. Mecham, T. A. Zawodzinski, J. E. McGrath, *Macromol. Symp.*, **175**, 387 (2001).
22. Z. Bai, L. D. Williams, M. F. Durstock, and T. D. Dang, *Polym. Prepr. (Am. Chem. Soc. Div. Polym. Chem.)*, **45**, 60 (2004).
23. T. D. Dang, Z. Bai, M. J. Dalton, and E. Fossum, *Polym. Prepr. (Am. Chem. Soc. Div. Polym. Chem.)*, **45**, 22 (2004).
24. S. Srinivasan, E. A. Ticianelli, C. R. Derouin, and A. Redondo, *J. Power Sources*, **22**, 359 (1988).
25. J. Kim, S. M. Lee, S. Srinivasan, and C. Chamberlin, *J. Electrochem. Soc.*, **142**, 2670 (1995).
26. P. Costamagna, C. Yang, A. Bocarsly, and S. Srinivasan, *Electrochim. Acta*, **47**, 1023 (2002).
27. T. E. Springer and J. D. Raistrick, *J. Electrochem. Soc.*, **136**, 1594 (1989).
28. *Impedance Spectroscopy*, J. R. MacDonald, Editor, Wiley & Sons, New York (1987).
29. M. Ciureanu, S. D. Mikhailenko, and S. Kaliaguine, *Catal. Today*, **82**, 195 (2003).
30. T. E. Springer, T. A. Zawodzinski, M. S. Wilson, and S. Gottesfeld, *J. Electrochem. Soc.*, **143**, 587 (1996).